Electron Spin Resonance of Alkali Atoms in Inert-Gas Matrices*†

C. K. JEN, V. A. BOWERS, E. L. COCHRAN, AND S. N. FONER
Applied Physics Laboratory, The Johns Hopkins University, Silver Spring, Maryland
(Received January 30, 1962)

The electron spin resonance spectra of alkali atoms (Li, Na, K, Rb, Cs) trapped in inert-gas matrices (Ar, Kr, Xe) at liquid-helium temperature have been observed. The principal hyperfine structure for each alkali atom follows very closely the pattern prescribed by the known hyperfine constants. Around the position of each hyperfine component, there is in most cases a multiple line structure, which is shown experimentally to be associated with multiple trapping sites in the particular matrix. Values of $\Delta A/A_0$ and Δg_J, tabulated in all cases to describe the matrix effects on the spin resonance, are found to depend upon the nature of the trapping site as well as the character of the matrix.

Matrix effects on the electron spin resonance spectra of trapped alkali atoms are treated theoretically by an approach similar to that used in a previous study of trapped hydrogen atoms. In contrast to the latter case, the effect of the repulsive interactions (Coulomb and exchange) is found to be very prominent for alkali atoms in inert-gas matrices. In this treatment, the repulsive energy is approximated by the corresponding part of the Lennard-Jones potential. A detailed calculation of the quantities $\Delta A/A_0$ and Δg_J has been carried out for the case of Li in Ar. Theoretical and experimental results for this case are in reasonable agreement assuming that the Li atoms are trapped in substitutional sites. There is as yet no satisfactory explanation for the phenomenon of multiple trapping sites for the alkali atoms.

I. INTRODUCTION

SINCE the alkali atoms are similar in many respects to the hydrogen atom, it was expected that the electron spin resonance (ESR) characteristics of these atoms in the trapped state would bear a strong resemblance to those of the hydrogen atom previously studied.[1,2] However, the fact that alkali atoms have more extensive charge distributions, higher polarizabilities, and a variety of nuclear spins affords a wider scope for the study of the interactions between simple free radical systems and their solid environment. In this paper, the ESR spectra of five alkali atoms have been examined individually in each of three inert-gas matrices at liquid-helium temperature.

II. EXPERIMENTAL

The experimental arrangement was similar to that reported previously,[1,2] the essential modification being the use of an oven as the source of atoms as shown in Fig. 1, rather than an electrical discharge. The oven temperature was adjusted to give a vapor pressure of about 0.05 mm Hg. The molecular beam of alkali atoms from the oven and beams of the selected inert gas from the matrix slits were codeposited on the liquid-helium-cooled sapphire rod. The ratio of matrix to alkali atoms in the input to the sapphire rod was typically of the order of 100:1. The number of alkali atoms in the sample as deduced from the intensities of the observed ESR lines was at least an order of magnitude lower than the calculated number of atoms incident on the sapphire rod. Although some of the atoms trapped in unsymmetrical environments, such as at crystalline imperfections or surface sites, may not have been observed because of excessive line broadening, the absence of pronounced dipolar broadening of the observed narrow lines (even at high alkali atom inputs) confirms the low atomic concentration in the sample and indicates that a large fraction of the alkali atoms were lost in the deposition process.

Observations were usually made at 4.2°K. To study the effects of temperature on the ESR spectra, a number of warmup experiments was attempted. Most of the warmup experiments were unsuccessful due to sudden degradation of the vacuum at temperatures where the matrix should have been stable, causing a rapid rise in temperature and premature loss of the sample. This experimental difficulty is probably due to the release of low-boiling-point impurities, principally

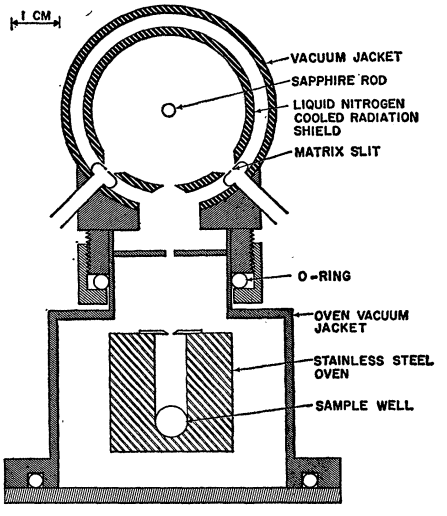

FIG. 1. Cross section of sample deposition system for alkali atoms and low-temperature cell.

* This work supported by the Bureau of Naval Weapons, Department of the Navy, under NOrd 7386.
† A part of this paper was presented at the Fifth International Symposium on Free Radicals, July 6–7, 1961, at Uppsala, Sweden.
[1] C. K. Jen, S. N. Foner, E. L. Cochran, and V. A. Bowers, Phys. Rev. **112**, 1169 (1958).
[2] S. N. Foner, E. L. Cochran, V. A. Bowers, and C. K. Jen, J. Chem. Phys. **32**, 963 (1960).

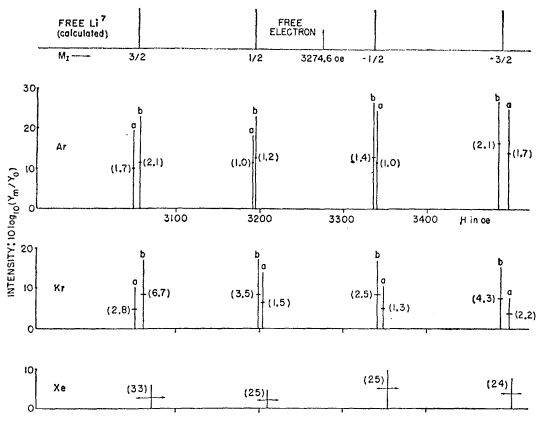

FIG. 2. A plot of ESR spectra for Li^7 in Ar, Kr, and Xe matrices at 4.2°K. Numbers in parentheses beside each line denote ΔH_{ms} (separation between maximum slope points in oersteds).

hydrogen, condensed on the walls of the liquid-helium Dewar.

III. RESULTS OF OBSERVATION

ESR observations of Li, Na, K, Rb, and Cs atoms were made in matrices of Ar, Kr, and Xe at liquid helium temperature. Figure 2 shows the observed spectra for Li^7 in Ar, Kr, and Xe matrices. Relative to the calculated line positions of the quartet hf spectrum for a free $Li^7(I=\frac{3}{2})$ atom, it is seen that the observed line positions for the trapped state are closely correlated with those of the free state. Also, corresponding to each line (designated by its M_I value at high magnetic fields) in the free state, two lines are observed for Li^7 in Ar, and similarly for Li^7 in Kr. A trace of one of the doubled lines for Li^7 in Ar is shown in Fig. 3. This phenomenon suggests the presence of multiple trapping sites analogous to that observed for H atoms[2] in Ar and in Kr. The broadening of the spectrum for Li^7 in Xe, indicated by the unresolved lines in Fig. 2, may be the result of hf broadening due to magnetic matrix nuclei (Xe^{129} and Xe^{131}), analogous to similar effects[2] for H in Xe. Finally, there is a noticeable shift of the corresponding spectral positions in the direction of somewhat higher magnetic fields as the matrix is changed first from Ar to Kr and then from Kr to Xe, indicating a shift to smaller electronic g values (g_J) as the size (or mass) of the matrix atom increases. This is in qualitative agreement with the results obtained for trapped H atoms.

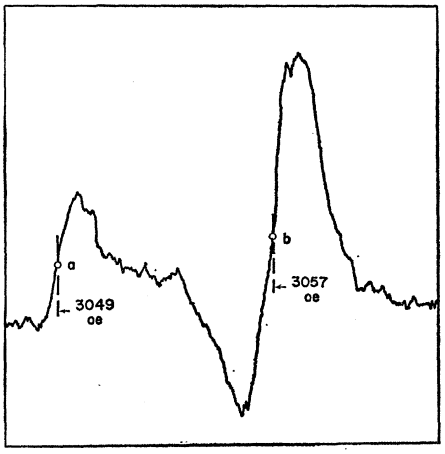

FIG. 3. A trace of $M_I=\frac{3}{2}$ hf lines for Li^7 in Ar matrix. Component (a) corresponds to $\Delta A>0$ and component (b) corresponds to $\Delta A<0$.

The intensity of a spectral line is represented in Fig. 2 as $10\log_{10}(Y_m/Y_0)$, where Y_m is the maximum amplitude of a derivative absorption curve and Y_0 is a reference amplitude. (Y_0 has a fixed value for these and other similar curves in this paper, roughly representing the limit of detectability.) If ΔH_{ms} is the line width in oersteds between maximum slope points, then the integrated intensity, which is proportional to $\Delta H_{ms}{}^2 Y_m$, is expected to be the same for all hf components in the ESR spectrum of an atomic species. Consequently, the quantity Y_m for a given spectral series should vary inversely as $\Delta H_{ms}{}^2$. The correspondence between this rule and the experimental data can be seen to be close in some instances and rather remote in others. The cause for this discrepancy in intensity distribution is not well understood.

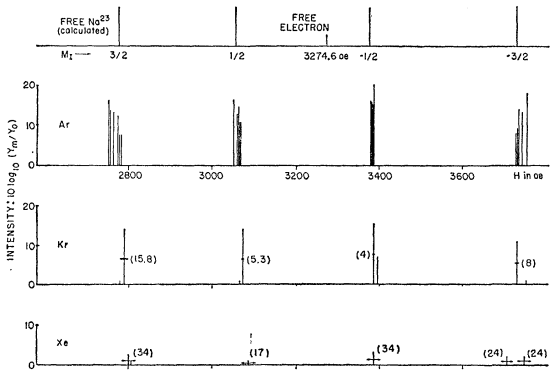

FIG. 4. A plot of ESR spectra for Na^{23} in Ar, Kr, and Xe matrices at 4.2°K. Numbers in parentheses beside each line denote ΔH_{ms}.

The general pattern set by the hf spectra of Li^7 in the inert-gas matrices is followed closely by the other alkali atoms. Figures 4–7 show, respectively, the observed results for Na^{23}, K^{39}, Rb^{85}, and Cs^{133} in Ar, Kr, and Xe matrices. A new feature, which is prominent in the spectra of Na, K, and Rb in the Ar matrix, is the presence of a structure of many lines at each M_I position, instead of only two lines as in the case of Li in Ar. The number of hf components in a group was as high as seven.

Some information on the nature of the trapping sites responsible for the multiple line structure in the ESR spectra can be obtained from studies on their temperature dependence. As mentioned in the experimental

section, most of the warmup experiments were vitiated by premature loss of the sample due to vacuum problems. Nevertheless, evidence for the discrete nature of the trapping sites was obtained in an experiment on Na^{23} in Ar. Figure 8 is the observed structure in the spectrum for $M_I=\frac{1}{2}$ at 4.2°K. In the warmup experiment, all components except *a* and *b* in Fig. 8 disappeared at about $T=36$°K, component *b* disappeared at about 38°K, and, finally, component *a* disappeared at about 40°K. Although the temperature range for these events was rather narrow, there was no ambiguity about the sequence and the distinct nature of the events. On the basis of this evidence, one can conclude that the observed spectrum corresponded to three or more trapping sites for Na atoms in the Ar matrix. One could also infer from this demonstration that the many-line spectra for K and Rb atoms (also possibly for the unresolved spectrum for Cs) in the Ar matrix should be identified with trapping in multiple sites.

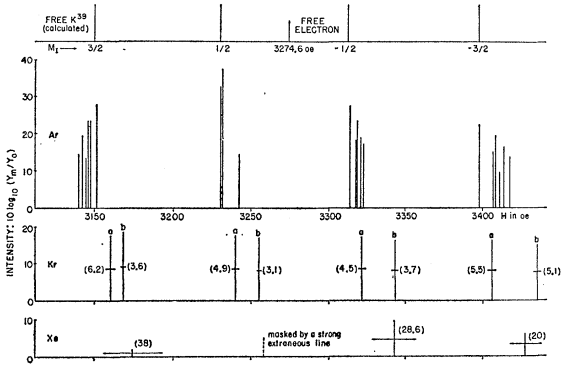

FIG. 5. A plot of ESR spectra for K^{39} in Ar, Kr, and Xe matrices at 4.2°K. Numbers in parentheses beside each line denote ΔH_{ms}.

In connection with the ESR observations on Li^7 and K^{39} atoms in an Ar matrix, it should be mentioned that the spectra for the less abundant species, Li^6 and K^{41}, were also observed. There were three hf components for Li^6 as expected for $I(Li^6)=1$ and four hf components for K^{41} as expected for $I(K^{41})=\frac{3}{2}$. In both cases, the line separations were consistent with the known hf coupling constants and the line intensities relative to those of Li^7 and K^{39} were in rough agreement with their natural abundances.

IV. CHANGES IN HYPERFINE PARAMETERS DUE TO MATRIX ENVIRONMENT

The spin Hamiltonian for an alkali atom in the $^2S_{\frac{1}{2}}$ state is

$$\mathcal{H}=g_J\beta\mathbf{J}\cdot\mathbf{H}+g_I\beta\mathbf{I}\cdot\mathbf{H}+A\mathbf{J}\cdot\mathbf{I}, \quad (1)$$

where the first two terms are the Zeeman energies in a magnetic field and the third term is the isotropic hf interaction energy. **J** and **I** are, respectively, the electronic and nuclear angular momenta in units of $\hbar$, g_J and g_I are the corresponding *g* factors in units of the Bohr magneton β, **H** is the magnetic field and *A* the isotropic hyperfine coupling constant. If the atom is trapped in a symmetric environment (as when surrounded symmetrically by inert-gas atoms), the atom is subject to an essentially centro-symmetric electrostatic field and the Hamiltonian for the trapped atom can still be describable by Eq. (1). Under these conditions, the hf coupling constant (A) and the electronic *g* factor (g_J) for the atom in the trapped state can be written as

$$\begin{aligned} A&=A_0+\Delta A, \\ g_J&=(g_J)_0+\Delta g_J, \end{aligned} \quad (2)$$

where A_0 and $(g_J)_0$ are parameters characteristic of the free atom and ΔA and Δg_J are the deviations from the free-atom parameters as a result of the matrix environment. It is the primary objective of this paper to determine and, wherever possible, to interpret the significance of ΔA and Δg_J for various alkali atoms in inert-gas matrices.

The quantities ΔA and Δg_J are determined by using the Breit-Rabi formula [which is the solution of Eq. (1)] with the usual selection rules, and using the differences between the measured values of the line positions and those predicted for a free atom. The data from any pair of lines belonging to the same spectral series should be sufficient to uniquely determine ΔA

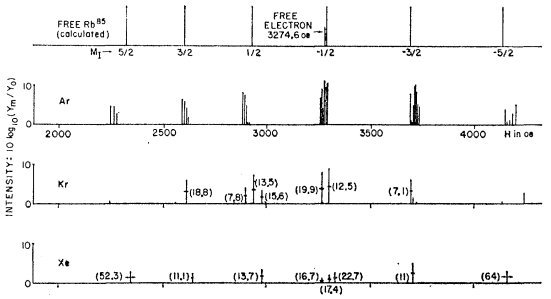

FIG. 6. A plot of ESR spectra for Rb^{85} in Ar, Kr, and Xe matrices at 4.2°K. Numbers in parentheses beside each line denote ΔH_{ms}.

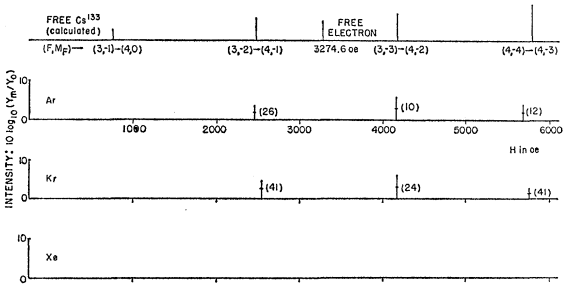

FIG. 7. A plot of ESR spectra for Cs^{133} in Ar, Kr, and Xe matrices at 4.2°K. Numbers in parentheses beside each line denote ΔH_{ms}. Lines in Xe were probably too weak and broad to be identifiable.

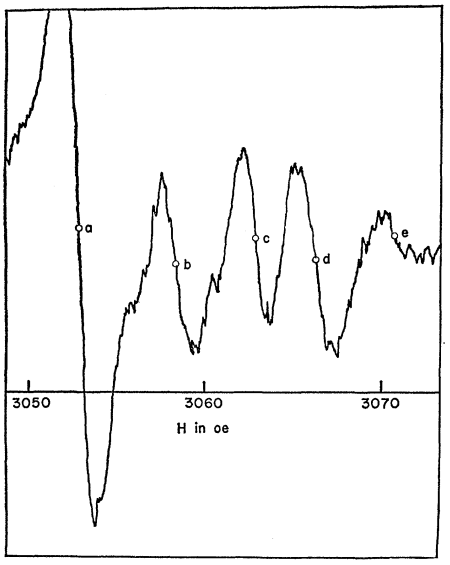

FIG. 8. A trace of $M_I=\frac{1}{2}$ hf lines for Na^{23} in Ar matrix at 4.2°K.

and Δg_J, and in principle these values should be identical with the results obtained by using any other pair of lines in the same series. If the results for ΔA and Δg_J obtained by using different pairs of lines do not agree within experimental error, it means that Eq. (1) is not a complete description of the situation and an added contribution, such as an anisotropic term, should be introduced. Small effects of this kind have been encountered in our observations, suggesting an anisotropic contribution to the hf energy due to slight asymmetries in the crystalline field. Since they are negligible for our present purposes, however, we shall simply use the average of all independent determinations of ΔA and Δg_J.

Table I lists the known values[3] of I, A_0/h, and $(g_J)_0$ for Li^7, Na^{23}, K^{39}, Rb^{85}, and Cs^{133}. Here A_0 is related to the zero-field hf splitting energy ΔW by $A_0=2\Delta W/(2I+1)$. The results of $\Delta A/A_0$ and Δg_J for all observed cases are given, respectively, in Tables II and III. It is seen in Table II that there are four cases (Li in Ar, Li in Kr, Na in Kr, and K in Kr) in which each hf component has two lines as a result of the matrix effect. One of these two sets is characterized by a positive shift in A ($\Delta A/A_0>0$) and the other by a negative

TABLE I. Values of I, A_0/h, and $(g_J)_0$ for the alkali atoms.[a]

	Li^7	Na^{23}	K^{39}	Rb^{85}	Cs^{133}
I	$\frac{3}{2}$	$\frac{3}{2}$	$\frac{3}{2}$	$\frac{5}{2}$	$\frac{7}{2}$
A_0/h (Mc/sec)	401.756	885.813	230.860	1011.912	2298.158
$(g_J)_0$	2.00231	2.00231	2.00231	2.00241	2.00258

[a] g_J (free electron) =2.00230. See reference 3.

[3] P. Kusch and V. W. Hughes, *Handbuch der Physik*, edited by S. Flügge (Springer-Verlag, Berlin, 1959), Vol. 37, Part 1, pp. 100 and 117.

TABLE II. Values of $\Delta A/A_0$ in percent for alkali atoms in inert-gas matrices.[a]

Matrix	Li	Na	K	Rb	Cs[b]
Ar	−1.6, 3.1 (2)	−0.9↔4.9 (6)	−0.4↔11.8 (6)	2.6↔8.4 (7)	0.5 (*u*)
Kr	−1.7, 2.2 (2)	−1.4, 2.0 (2)	−1.2, 6.6 (2)	−0.56↔6.9 (3)	−0.9 (*u*)
Xe	−1.2 (*u*)	−1.3 (*u*)	1.7 (*u*)	−1.6 (*u*)	···

[a] The number in parentheses denotes the maximum number of lines in a group defined by M_I. The symbol (*u*) denotes that the lines in a group defined by M_I are unresolved.
[b] Denotes value computed from $M_I=-3/2$ and $M_I=-5/2$ transitions (high-field notation).

shift in A ($\Delta A/A_0<0$). In other cases, where there are higher orders of multiplicity (Na in Ar, K in Ar, Rb in Ar, and Rb in Kr), the lines are not individually classified because of difficulties of identification. Nevertheless, the spread of the lines in each M_I group produces a corresponding spread of $\Delta A/A_0$, the range of which is indicated. In each of the remaining cases, there is a broad and unresolved line at each M_I position which can be characterized by a value of $\Delta A/A_0$ corresponding to the peak of the broad line.

The results for Δg_J in Table III illustrate the usual situation for trapped radicals in that almost all Δg_J values are negative. As a rule, for a particular matrix, a spectrum with $\Delta A>0$ yields a larger negative shift in g_J than one with $\Delta A<0$. Also, for a given atom, an inert-gas matrix with a higher molecular weight consistently causes a larger negative shift in g_J.

V. THEORY

A. General Description

The Zeeman and hyperfine energies of an alkali atom in the free state are described by the solution of Eq. (1) with the known constants A_0, $(g_J)_0$, and I. When the atom is trapped in a matrix, there are various interactions with the surrounding matrix particles which cause perturbations of the Zeeman and hyperfine energies. In order to calculate these perturbations, one has to know or assume the physical configuration of the trapping site. In the case of a hydrogen atom,[2] one can assume that the atom may reside in an interstitial as well as a substitutional site without appreciably distorting the lattice. An alkali atom, however, because of its larger size cannot occupy an interstitial site, but may be accommodated in a substitutional site with a degree of lattice distortion depending on both the alkali atom and the matrix. In the case of the larger alkali atoms, Rb and Cs, the distortions involved in fitting the atom into a substitutional site may be so large that this description of the trapping site is not applicable. In addition, there is the possibility that atoms may be trapped in amorphous regions, and on the surfaces or edges of the matrix microcrystals.

In order to avoid the immediate necessity of choosing

a certain site configuration and the difficulties of dealing with many particle interactions, we will treat the comparatively simpler problem of a pair of atoms (one alkali and one inert gas) and assume that the law of additivity holds true for any number of pairs, as Adrian has done in his treatment of the hydrogen atom problem.[4] We will further assume, also following Adrian, that the results from the long- and short-range interactions can be treated separately and added together to form the net effect. In considering the short-range interactions for the alkali atoms, it will be shown later that it is very essential to include, in addition to the overlap (Pauli exclusion) effect, perturbation effects due to large distortions of the electronic wave function.

Let the subscript L denote an alkali atom and M a matrix atom. Then the total Hamiltonian, in the absence of magnetic field, can be written as

$$\mathcal{H}=\mathcal{H}_L+\mathcal{H}_M+\mathcal{H}_{\rm int}+\mathcal{H}_{\rm hf}, \tag{3}$$

where $\mathcal{H}_L$ and $\mathcal{H}_M$ are respectively, the energies of the isolated alkali and matrix atoms (not considering the hf energy), $\mathcal{H}_{\rm int}$ is the interaction energy between the atoms (containing all electrostatic energy terms between the charges of different atoms), and $\mathcal{H}_{\rm hf}$ is the hyperfine energy. The quantity $\mathcal{H}_{\rm hf}$ can be written as

$$\mathcal{H}_{\rm hf}=(8\pi/3)g_J g_I \beta^2 \textstyle\sum_i \delta(\mathbf{r}_i)\mathbf{J}_i\cdot\mathbf{I}, \tag{4}$$

where δ is the Dirac delta operator and $\mathbf{r}_i$ is the position vector of the ith electron having its origin at the alkali nucleus. We will now examine the hf energy values corresponding to the perturbation Hamiltonian

$$\mathcal{H}'=\mathcal{H}_{\rm int}+\mathcal{H}_{\rm hf}, \tag{5}$$

for large and small values of the internuclear distance.

B. Effect of Long-Range Interactions

If the internuclear distance R is sufficiently large, then $\mathcal{H}_{\rm int}$ becomes the well-known van der Waals interaction energy. The effect of $\mathcal{H}_{\rm int}$ on the hf energy for this case can be calculated in exactly the same way as for the hydrogen atom with the following result[4]:

$$\Delta W_{\rm hf}=-W_{\rm hf}((2/E_L)+[1/(E_L+E_M)])E_V, \tag{6}$$

where $W_{\rm hf}$ is the unperturbed hf energy of the alkali atom, $\Delta W_{\rm hf}$ is the change in the hf energy due to the van der Waals interaction, E_L is the mean energy of the excited states of the alkali atom, E_M is the same for the matrix atom, and E_V is the van der Waals (or dispersion) energy. The asymptotic expression for E_V at large values of R is[5,6]

$$E_V=-C/R^6, \tag{7}$$

where C can be calculated approximately from the well-known expression[5]

$$C=\frac{3}{2}\left|\frac{E_L E_M}{E_L+E_M}\right|\alpha_L\alpha_M, \tag{7a}$$

in which α is the electric polarizability of the atom. The coefficient C can also be evaluated from atomic scattering experiments.[6]

Since the mean energies appearing in Eq. (6) are intrinsically negative and E_V is also negative by Eqs. (7) and (7a), $\Delta W_{\rm hf}$ is negative for a positive value of $W_{\rm hf}$. Quantitatively, the value of $\Delta W_{\rm hf}/W_{\rm hf}$ for an alkali atom is an order of magnitude larger than that of the hydrogen atom essentially because of the very large polarizabilities of the alkalis.

TABLE III. Values of $-100\Delta g_J$ for alkali atoms in inert-gas matrices.[a]

Matrix	Li	Na	K	Rb	Cs[b]
Ar	0.05, 0.13 (2)	0.05↔0.21 (6)	0.08↔0.37 (6)	−0.85↔0.89 (7)	−0.25 (*u*)
Kr	0.36, 0.57 (2)	0.45, 0.93 (2)	0.59, 1.74 (2)	0.65↔1.07 (3)	0.11 (*u*)
Xe	1.09 (*u*)	0.98 (*u*)	1.66 (*u*)	2.02 (*u*)	...

[a] See note a of Table II.
[b] See note b of Table II.

C. Effect of Short-Range Interactions

If the internuclear distance R is sufficiently small, the electronic wave functions of the two atoms will overlap considerably. This implies a violation of the Pauli exclusion principle, leading to a perturbation of the wave functions and a change in the hf energy. In addition, particularly for the alkali atoms, the wave functions are strongly distorted by the Coulomb and exchange interactions associated with the energy terms of $\mathcal{H}_{\rm int}$ in Eq. (5). We can examine these effects by following through the usual perturbation calculations.

First, assume the total ground-state wave function (including spin) is antisymmetrized for all electrons in both atoms. Let ψ_0 denote such a wave function. Then the first order perturbation treatment for $\mathcal{H}'$ in Eq. (5), retaining only the term linear in $\mathcal{H}_{\rm hf}$, gives simply

$$W_1'=(\psi_0|\mathcal{H}_{\rm hf}|\psi_0), \tag{8}$$

the explicit form of which will be given later. For the second-order perturbation, we need the wave functions in the excited state, such as ψ_K in the Kth state, which can be built up in the determinantal form by combining, for instance, the excited-state wave function of the

[4] F. J. Adrian, J. Chem. Phys. **32**, 972 (1960).

[5] J. O. Hirschfelder, C. F. Curtiss, and R. B. Bird, *Molecular Theory of Gases and Liquids* (John Wiley & Sons, Inc., New York, 1954), p. 964.

[6] H. S. W. Massey and E. H. S. Burhop, *Electric and Ionic Impact Phenomena* (Oxford University Press, New York, 1952), p. 397.

alkali valence electron with the ground-state wave functions of all the other electrons. The second-order perturbation gives in the usual manner,

$$W_2'=\sum_K{}' \frac{(\psi_0|\mathcal{H}_{\rm int}+\mathcal{H}_{\rm hf}|\psi_K)(\psi_K|\mathcal{H}_{\rm int}+\mathcal{H}_{\rm hf}|\psi_0)}{W_0{}^0-W_K{}^0}, \quad (9)$$

where the prime on the summation sign indicates the ground state ψ_0 is omitted in the summation and W^0 is the unperturbed energy in the state defined by its subscript. By using the mean value for the energy denominator, a procedure commonly employed under similar situations, and by retaining only the terms linear in $\mathcal{H}_{\rm hf}$, we have

$$W_2'=-(2/E_L)(\psi_0|\mathcal{H}_{\rm int}|\psi_0)(\psi_0|\mathcal{H}_{\rm hf}|\psi_0), \quad (10)$$

where E_L is the mean energy for the excited states of the alkali atom, $\langle W_0{}^0-W_K{}^0\rangle$, (assumed to be the same as in Eq. (6) even though different kinds of averaging are involved). In obtaining Eq. (10) from Eq. (9), it can be shown that the term $(\psi_0|\mathcal{H}_{\rm int}\mathcal{H}_{\rm hf}|\psi_0)$ is vanishingly small.

The sum of the first- and second-order perturbations $(W'=W_1'+W_2')$ is

$$W'=(\psi_0|\mathcal{H}_{\rm hf}|\psi_0)\left\{1-\frac{2}{E_L}(\psi_0|\mathcal{H}_{\rm int}|\psi_0)\right\}. \quad (11)$$

The first term in Eq. (11) can be written approximately as[4]

$$(\psi_0|\mathcal{H}_{\rm hf}|\psi_0)\doteq W_{\rm hf}\{1+\textstyle\sum_M(\psi_L|\psi_M)^2\}, \quad (12)$$

where ψ_L is the wave function of the unpaired s electron of the alkali atom and ψ_M is the wave function of the Mth electron of the matrix atom. Combining Eq. (11) and Eq. (12) and letting $\Delta W_{\rm hf}=W'-W_{\rm hf}$, we have for the net change of the hf energy, neglecting high-order terms,

$$\Delta W_{\rm hf}=W_{\rm hf}\left\{\sum_M(\psi_L|\psi_M)^2+\frac{2}{|E_L|}(\psi_0|\mathcal{H}_{\rm int}|\psi_0)\right\}. \quad (13)$$

It is seen that the first term on the right-hand side of Eq. (13) is the change in hf energy due to the overlap effect. This effect is brought about by the nonorthogonality between the valence-electron wave function of the alkali atom and the electronic wave functions of the matrix atom. This is the term considered by Adrian in his treatment of the hydrogen atom problem. The second term represents the change in hf energy due to the effect of $\mathcal{H}_{\rm int}$. The term $(\psi_0|\mathcal{H}_{\rm int}|\psi_0)$ stands for the *net* contribution of the Coulomb and exchange interaction energies.[7] When the net value is positive, it represents a repulsive potential energy. Hence, the second term should be interpreted as the change in hf energy from the distortion of the valence-electron wave function caused by this repulsive potential.

[7] See reference 5, p. 937.

By performing a second order perturbation calculation of the spin-orbit interaction in a manner similar to Adrian's work except for the consideration of the repulsive effect, we have for the shift of the electronic g factor

$$\Delta g_J\doteq-\frac{8}{9}\frac{\lambda_{p\sigma}}{E_L}(\psi_L|\psi_{p\sigma})^2\left\{1+\frac{2}{|E_L|}(\psi_0|\mathcal{H}_{\rm int}|\psi_0)\right\}, \quad (14)$$

where $\psi_{p\sigma}$ is the outermost $p\sigma$ orbital of the matrix atom and $\lambda_{p\sigma}$ is the spin-orbit splitting constant of the same orbital.

D. Approximation by the Lennard-Jones Potential

Instead of attempting some formidably difficult calculations of the repulsive potential, a reasonable approximation can be achieved by using the Lennard-Jones potential which is written as[8]

$$\phi(R)=4\epsilon\{(\sigma_{LM}/R)^{12}-(\sigma_{LM}/R)^6\}, \quad (15)$$

where σ_{LM} is the "collision diameter" between a pair of atoms (molecules) labeled as LM, and ϵ is the depth of the potential well. By identifying the second term on the right-hand side of Eq. (15) as the van der Waals energy in Eq. (7) we can equate the first term to the repulsive energy which is needed in Eqs. (13) and (14). Thus, we have

$$E_V=-4\epsilon(\sigma_{LM}/R)^6 \quad (16)$$

and

$$(\psi_0|\mathcal{H}_{\rm int}|\psi_0)=4\epsilon(\sigma_{LM}/R)^{12}. \quad (17)$$

The parameter σ_{LM} can be estimated either from gas kinetic data or from certain empirical relations.[9,10] The parameter ϵ can then be derived either from a theoretical expression for E_V as in Eq. (7a) or from atomic scattering experiments.[6] The knowledge of both σ_{LM} and ϵ leads to the repulsive energy by Eq. (17).

E. Calculation of the Matrix Effect for Li in Ar

We can now calculate $\Delta A/A_0$ for an alkali atom by noting that

$$\Delta A/A_0=\Delta W_{\rm hf}/W_{\rm hf}, \quad (18)$$

and using Eqs. (6) and (13) with the aid of Eqs. (16) and (17). The quantity Δg_J is calculated from Eq. (14) with the use of Eq. (17). We will take Li in Ar as the representative case to study not only because it is theoretically the simplest but also because it is experimentally the most cleancut.

For the calculation of the overlap integrals, Slater orbitals[11] have been used for the Li atom and Hartree's

[8] See reference 5, p. 32.

[9] L. Pauling, *The Nature of the Chemical Bond* (Cornell University Press, Ithaca, New York, 1960), 3rd ed., p. 263.

[10] J. O. Hirschfelder and M. A. Eliason, Ann. Acad. Sci. (N.Y.) **67**, 451 (1957).

[11] L. Pauling and E. B. Wilson, Jr., *Introduction to Quantum Mechanics* (McGraw-Hill Book Company, Inc., New York, 1935), p. 248.

tabulated results for the Ar atom.[12] For the van der Waals constant C in Eq. (7) for Li and Ar, the experimental value $C=188\times10^{-60}$ erg cm^6 by Rosin and Rabi[13] is probably too low in view of the more recent work by Rothe and Bernstein[14] on K-Ar and Cs-Ar. Instead of extrapolating the results by an arbitrary procedure, we prefer to calculate for the value of C from Eq. (7a) with the latest value $\alpha_L=20\times10^{-24}$ cm^3 for the Li atom[15] in addition to the usual value $\alpha_M=1.68\times10^{-24}$ cm^3 for the Ar atom. This yields the result: C (calculated)$=237\times10^{-60}$ erg cm^6 for Li and Ar. This value happens to be very close to C(extrapolated)$=237\times10^{-60}$ erg cm^6 if we raise the result of Rosin and Rabi by a factor 1.28 as found by Rothe and Bernstein for K and Ar. The value of σ_{LM} between Li and Ar is taken to be

$$\sigma_{LM}=\bar{r}_{\mathrm{Ar}}+\langle r\rangle_{\mathrm{Li}}, \tag{19}$$

where $\bar{r}_{\mathrm{Ar}}=1.71$ Å, being the gas kinetic collision radius for argon,[16] and $\langle r\rangle_{\mathrm{Li}}=2.10$ Å, being the mean radius of the Li $2s$ electron averaged over its orbital.[11] The value of 2.10 Å for $\langle r\rangle_{\mathrm{Li}}$ is consistent with an empirical rule proposed by Pauling[9]: $\langle r\rangle_{\mathrm{Li}}=r_{\mathrm{Li}}$(covalent radius) $+0.8=2.14$ Å.

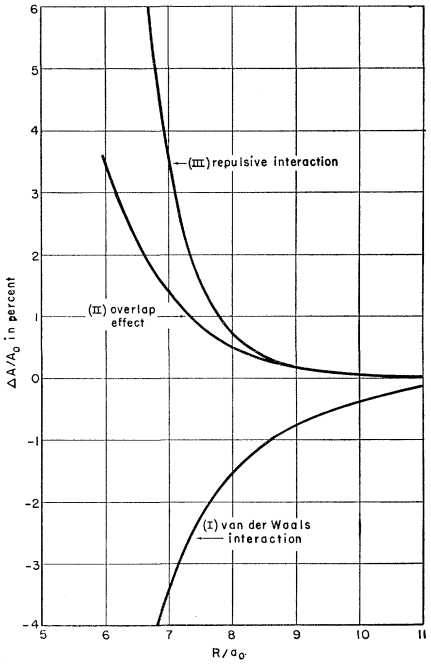

FIG. 9. Calculated contributions to $\Delta A/A_0$ for Li in Ar matrix as a function of R/a_0 (a_0=Bohr radius of the hydrogen atom): (I) Effect of van der Waals interaction; (II) effect of overlap of atomic wave functions; (III) effect of repulsive interaction. All values of $\Delta A/A_0$ are for a single pair of atoms.

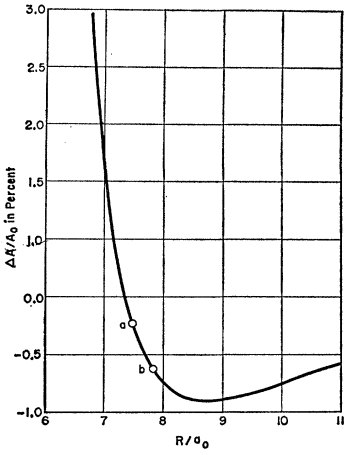

FIG. 10. Sum of all calculated contributions to $\Delta A/A_0$ for Li in Ar matrix as a function of R/a_0. Values of $\Delta A/A_0$ are for a single pair of atoms. The letters a and b denote spectral systems in Fig. 2.

The results of the calculation for the three-component contributions (overlap, repulsive interaction, van der Waals interaction) to $\Delta A/A_0$ are shown in Fig. 9. It is seen that the overlap effect varies much more slowly with respect to R than the van der Waals effect. The algebraic sum of these two contributions, when the repulsive interaction is not included, would give a continuously increasing negative value for $\Delta A/A_0$ as R decreases, contrary to the experimental result. On the other hand, however, when the repulsive interaction is taken into consideration, the repulsive effect balances the van der Waals effect roughly at $R=\sigma_{LM}$(3.81 Å or $7.20a_0$), which is the crossover point for the Lennard-Jones potential. The effect of the overlap contribution, which should be included for the total effect, merely pushes the crossover point to a somewhat larger value than σ_{LM}.

The over-all value for $\Delta A/A_0$ as a function of R is shown in Fig. 10 and the calculated value for Δg_J is shown in Fig. 11. The effect of the repulsive interaction on Δg_J turns out to be rather negligible, since the second term in Eq. (14) is much smaller than unity in the range of interest.

In comparing the experimental results, as tabulated in Tables II and III, with the calculated results in Figs. 10 and 11, it is necessary to know the number of matrix atoms surrounding an alkali atom (which is equal to the number of atom pairs). We will make the assumption that only the nearest neighbors contribute significantly to the matrix effect and that all the nearest neighbors are equivalent (equal internuclear distances from the alkali atom). We will assume 12 nearest neighbors, as for a normal substitutional site in a face-centered cubic lattice. Dividing the tabulated results of $\Delta A/A_0$ for Li in Ar in Table II by 12, we have plotted the resulting values for spectral series a and b on the $\Delta A/A_0$ curve in Fig. 10. Corresponding values of Δg_J in Table III, divided by 12, are also plotted in Fig. 11, using the internuclear distances

[12] D. R. Hartree and W. Hartree, Proc. Roy. Soc. (London) A166, 450 (1938).
[13] S. Rosin and I. I. Rabi, Phys. Rev. 48, 373 (1935).
[14] E. W. Rothe and R. B. Bernstein, J. Chem. Phys. 31, 1619 (1959).
[15] A. Salop, E. Pollack, and B. Bederson, Phys. Rev. 124, 1431 (1961).
[16] See reference 5, p. 205.

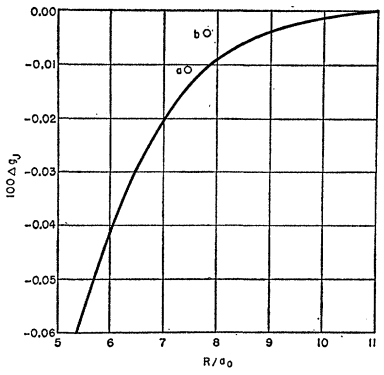

FIG. 11. Calculated Δg_J for Li in Ar matrix as a function of R/a_0. Values of Δg_J are for a single pair of atoms. The letters a and b denote spectral systems in Fig. 2.

already fixed in Fig. 10. The points a and b in Fig. 11 do not fall on the calculated curve, but the over-all agreement between the calculated and experimental results may be considered as reasonably close (particularly for point a), considering the approximate nature of the theory and experimental uncertainties in the g-shift determination.

From the plotted points in Fig. 10, the internuclear distance for site a is $R_a=7.4_5a_0$ and the corresponding distance for site b is $R_b=7.8_2a_0$ as compared with the distance $R_0=7.0_9a_0$ between the nearest neighbors in an argon lattice. The internuclear distances for both site a and site b are, within the accuracy of the calculation, close to the distance for a substitutional site in argon. This suggests that both a and b may arise from discrete, slightly distorted substitutional sites in argon, the discrete nature of the sites being a consequence of lattice energy relationships. An alternative possibility is that only one of the sites is a substitutional site (theory would favor site a because of the closer agreement), and the other site is unspecified in the absence of further information.

VI. EFFECT OF MATRIX ON THE WIDTH OF SPECTRAL LINES

The effect of the matrix on the alkali atoms is also revealed in the shapes and widths of the hf spectral lines. Under the conditions of the present studies, the intensity distribution of a spectral line is in most cases approximately Gaussian. This implies that the anisotropic effect on line broadening is relatively small, since anisotropy usually produces asymmetric line shapes.

A spectral linewidth can be considered the result of three effects: (1) spin-lattice relaxation, (2) dipolar interaction, and (3) crystalline field. In addition, hyperfine broadening due to magnetic nuclei among the matrix particles may be present, as in the case of alkali atoms trapped in Xe. The effect of spin-lattice relaxation is in general very complicated, but in principle can be eliminated from consideration by using sufficiently low microwave intensities below "saturation." The effect of dipolar interaction is quite negligible if the radical concentration is very low (e.g., below about 0.01%). The effect of the crystalline field is regarded in the present studies as the dominant source of line broadening and will now be examined in some detail.

The crystalline field effect on line broadening can be approximately described (accurately for Gaussian distributions) by

$$\Delta H_{ms}^2=\Delta H_0^2+\Delta H_A^2, \tag{20}$$

where ΔH_0 is the broadening due to all crystalline effects which are unrelated to hf interactions (e.g., nonuniform g_J shifts) and ΔH_A is the hf broadening due to lack of uniformity of the crystalline field. Hf broadening due to nonuniformity of the crystalline field can arise, for example, because one trapping site may be slightly different in size from another, even though both have identical symmetry. If δA is the Gaussian measure of the statistical *variation* of A (δA is different from ΔA, which is the *average* shift of A), then ΔH_A can be seen to be equal to $M_I\delta A$ when measured in magnetic field units.

Figure 2 shows the hf spectra of Li^7 with the ΔH_{ms} values indicated for each line. It is seen that the linewidths generally increase with higher M_I value. The dependence of the linewidth on M_I decreases as the atom is trapped in progressively heavier matrices. This pattern of linewidth variation holds roughly for all the alkali atoms, and is consistent with the results predicted by Eq. (20). Table IV shows the numerical values of the parameters ΔA, δA, and ΔH_0 for the example of Li^7 in Ar.

It is seen that although the two sites are well defined by their ΔA values, which are widely separated from each other, there is a spread of the A constant (δA) indicating lack of complete uniformity of the matrix in which the Li atoms are trapped. Lack of uniformity of the matrix sites may be, in part, the result of the cold-deposition procedure used in preparing the samples. This inhomogeneity could conceivably be reduced by subjecting the sample to a careful annealing process.

VII. MULTIPLE TRAPPING SITES

The phenomenon of multiple trapping sites has been experimentally demonstrated in the case of Na atoms in an argon matrix (Sec. III). It is believed that the same phenomenon is present in all cases where there are multiple hf spectra. However, we are as yet unable to formulate a physical model which is adequate to explain the *discrete* nature of the multiple trapping sites

TABLE IV. ΔA, δA, and ΔH_0 for Li^7 in Ar matrix.[a]

hf spectrum	ΔA (oe)	δA (oe)	ΔH_0 (oe)
a	+4.44	0.49	0.88
b	−2.29	0.61	1.03

[a] A_0 (free Li^7) = 143.19 oe.

for alkali atoms in inert-gas matrices. It is not clear why there should be several discrete trapping sites for an alkali atom in an inert-gas matrix, and, in particular, why this effect should be so pronounced for Na, K, and Rb in argon. There is the possibility that several discrete sites could represent different distortions of the substitutional site. We do not have sufficient knowledge of the lattice dynamics involved to give a definite answer to this question. There is also the possibility of atom trapping on microcrystalline surfaces, at crystalline defects, or in amorphous regions of the solid. The crystalline fields for atom trapping on the surface or at defects would be anisotropic and the random orientation of the microcrystals would be expected to smear the lines rather than give the observed narrow lines. In the case of trapping in amorphous regions, the nonreproducibility of the environment would be expected to result in a broad line rather than a discrete set of lines. The explanation of this phenomenon will require further experimental and theoretical studies.

VIII. EXTRANEOUS SPECTRA

In addition to the spectra directly identified with trapped alkali atoms, a number of unidentified spectra have also been observed in our experiments. In almost all experiments a strong line was observed near the free-electron-resonance position, with slight variation in spectral position depending on the alkali atom used. There was no obvious correlation between this line and the known resonance line for conduction electrons in the alkali metal. A second type of spectrum of unknown origin was a pattern of moderately closely spaced lines in the vicinity of the free electron position. These may be due to impurity paramagnetic species or, possibly, to alkali atom aggregates. A third type of spectrum consisting of many broad lines scattered all over the spectral range resulted from the exposure of the sapphire rod to alkali atoms in previous experiments. The spectrum grew in intensity with successive experiments for a particular alkali atom and was completely different for different alkali atoms. The spectrum is associated with stable paramagnetic centers generated in the sapphire rod. It was found that this spectrum was not drastically reduced in intensity even by the abrasive removal of a surface layer of sapphire 1/100 mm in thickness.

IX. CONCLUSIONS

The matrix effects of the inert gases on the ESR spectra of trapped alkali atoms were, as expected, very similar to but much larger than corresponding effects on trapped hydrogen atoms. The occurrence of high order multiplicities of trapping sites for certain alkali-matrix combinations has introduced a new and interesting phenomenon for which a satisfactory explanation is needed. A theoretical approach taking into account repulsive interactions as well as the overlap and van der Waals interactions has been developed for the calculation of matrix effects on the ESR spectra of alkali atoms. For the case treated in detail, Li in Ar, the theoretical and experimental results are in good agreement if the Li atoms are assumed to be trapped in substitutional sites. Studies of the widths of the spectral lines indicate a lack of complete uniformity of the matrix sites, possibly due to the cold-deposition procedure used.

ACKNOWLEDGMENT

The authors are indebted to Dr. F. J. Adrian for many helpful discussions.